Available online at www.sciencedirect.com
SCIENCE DIRECT
ELSEVIER
Icarus 171 (2004) 219–228
ICARUS
www.elsevier.com/locate/icarus

2002 Leonid storm fluxes and related orbital elements

Josep M. Trigo-Rodríguez [a,*], Jordi Llorca [b,c], Esko Lyytinen [d], Jose Luis Ortiz [e], Albert Sánchez Caso [f], Carles Pineda [g], Sebastià Torrell [h]

[a] *Astrobiology Center, Institute of Geophysics and Planetary Physics, University of California, Los Angeles, CA 90095-1567, USA*
[b] *Departament Química Inorgànica, Universitat de Barcelona, Marti i Franques 1-11, 08028 Barcelona, Spain*
[c] *Institut d'Estudis Espacials de Catalunya, Edifici Nexus, Gran Capità 2-4, 08034 Barcelona, Spain*
[d] *Kehäkukantie 3 B, 00720 Helsinki, Finland*
[e] *Instituto de Astrofísica de Andalucía (CSIC), PO Box 3004, 18080 Granada, Spain*
[f] *Gualba Observatory, Minor Planet Center Code 442, Spain*
[g] *Observatori de l'Alt Empordà, Minor Planet Center Code J91, Spain*
[h] *Grup d'Estudis Astronòmics GEA, Spain*

Received 3 April 2003; revised 4 March 2004

Available online 19 June 2004

Abstract

We report here the observation of the first peak belonging to the 2002 Leonid meteor storm made during the night of November 18–19, 2002. This feature, produced by a 7-revolution dust trail, was observed from several photographic stations of the Spanish Photographic Meteor Network (SPMN) and one video station operated from the Instituto de Astrofísica de Andalucía (IAA) in an intensive campaign from the ground working in collaboration with the 2002 Leonid MAC mission. We used photography, slow-scan Charge Coupled Devices (CCD) and video CCD-imaging techniques to deduce the meteoroid flux density profiles in different ranges of masses. Additionally, we present multi-station work, developed during the storm, that allows us to deduce the orbital elements of ten meteoroids associated with this dust trail. We have found a clear similarity between their orbits and the one belonging to a theoretical orbit for particles ejected from 55P/Tempel–Tuttle in 1767.

Keywords: Meteors; Meteoroids; Orbits; Comets; Leonids; 55P/Tempel–Tuttle

1. Introduction

This paper presents the results from photographic, video, charge coupled devices (CCDs) and visual monitoring of the meteoric activity during the 2002 Leonid storm. We developed this task on the basis of the stations and infrastructure provided by members and collaborators of the Spanish Photographic Meteor Network (SPMN). Since 1997 this network has been dedicated to studying interplanetary matter under the auspices of three universities (Universitat Jaume I, Universitat de Barcelona and Universitat de València), the Institute for Space Studies of Catalonia (IEEC) and is also supported by the Instituto de Astrofísica de Andalucía (IAA) and the El Arenosillo Observatory of the Spanish National Institute for Aerospace Techniques (INTA-CEDEA). On this occasion we collaborated from the ground with the 2002 Leonid MAC mission aircraft-studies directed by Dr. Peter Jenniskens (NASA/Ames). Amateurs also participate in our network, taking into account that the systematic observation of meteors using photographic, video and CCD techniques has become one of the rare fields in astronomy in which amateurs can work together with professionals and make important contributions to science.

When the Earth intercepts a dust trail, an important influx of cometary matter reaches the Earth and produces extraordinary meteor storms (Kresak, 1993). Nowadays, meteor storms are rather unusual events (Jenniskens, 1996), but during the formation of the Earth, the interplanetary cloud of dust was at least 100,000 times as dense as it is now (Delsemme, 2000). Therefore, it was probably a very important source of prebiotic material for the first billion years of the early Earth (Jenniskens et al., 2000). Leonid storms

* Corresponding author.
E-mail address: jtrigor@ucla.edu (J.M. Trigo-Rodríguez).

0019-1035/$ – see front matter
doi:10.1016/j.icarus.2004.03.020

produced by Comet 55P/Tempel–Tuttle provide us with an excellent way to test these ideas. Monitoring the sky using modern techniques allows us to register incoming meteors in order to study the amount of matter reaching the Earth during these processes by deducing the population index and the flux number density of the incoming particles.

In fact, during the years of Comet 55P/Tempel–Tuttle's return to perihelia, young meteoroid clouds appear, producing meteor outbursts (Yeomans et al., 1996; Asher, 1999; Brown, 1999; Brown and Arlt, 2000). Probably the most detailed information about the cometary mass entering the terrestrial atmosphere during these unusual events comes from radar observations. These allow us to derive the meteoroid mass distribution as a function of time from where the size and spatial density of the trails intercepting the Earth are deduced (Simek and Pecina, 2000, 2001).

In addition to radar studies, optical research using photography, video or CCD techniques is very valuable to probe deeper into the properties of these cometary meteoroids and determine their origin (Brown et al., 2002). Electro-optical observations provide us with valuable information about the radiant and the orbital elements with greater accuracy than other techniques. Until 1997 all optical studies of Leonid activity were obtained from visual observations even though photographs of the 1966 Leonid storm are also available (Milon, 1967). In previous works (Trigo-Rodríguez, 2000; Trigo-Rodríguez et al., 2001, 2002), we derived the spatial densities of the shower during this cometary return from visual observations compiled in the Visual Meteor Database of the International Meteor Organization (IMO) and also from photographs taken by the Spanish Photographic Meteor Network in the period 1994–1998 and by several astrophotographs taken during the 1966 Leonid storm. Here we present spatial densities derived from photographs, CCD and video registers of probably one of the last important Leonid storms of the 21st century (McNaught and Asher, 1999, 2001; Lyytinen and Van Flandern, 2000; Lyytinen et al., 2001).

The stations participating in our network worked from the ground in common atmospheric fields in order to obtain stereographic images of the meteors. In exactly the same way as other European teams that selected Spain as the focus of their 2002 observation campaigns, the majority of our stations were placed in the Southwest of Spain (Andalusia). This decision was guided by statistical predictions on the weather in November. Unfortunately, generalized bad weather in Spain and Portugal made it impossible to carry out a joint effort between these teams and it prevented a detailed study of the meteoroids presumably associated with the 1767 dust trail from being carried out (McNaught and Asher, 2002). Fortunately a small part of our network working from Catalonia was able to observe the storm under excellent skies, providing double-station images of Leonid meteors. They are especially valuable because this kind of work was impeded almost completely in other regions due to these unfortunate weather conditions.

From the common images of a same meteor from two photographic stations we can determine its real trajectory in the atmosphere, its radiant and, once the velocity has been deduced from accurate rotating shutters, the heliocentric orbit of the progenitor particle. Detailed orbital analyses are of special interest because precise information on orbital elements of Leonid meteoroids is relatively scarce. In fact, only 29 well-determined orbits were available in the period 1938–1985 (Lindblad et al., 1993; Wu and Williams, 1996). Then Betlem et al. (1997) and Shiba et al. (1999) obtained additional data for the 1995 and 1996 apparitions, respectively, and Betlem et al. (1999) used double-station meteor work to calculate 75 very precise orbits of meteoroids producing the 1998 Leonid outburst. The 1999 Leonid storm was also observed from the south of Spain by the same team (Betlem et al., 2000) and detailed data was obtained on 47 Leonid storm meteoroids. Recently, the origin of the 1999 Leonid storm was confirmed by our team as having been produced by a narrow dust trail ejected in 1899 from the 55P/Tempel–Tuttle (Trigo-Rodríguez et al., 2002).

In general, precise orbits and trajectories of meteors provide important clues with which to gain further insight into the orbital dynamics of meteoroids and the physical properties during atmospheric interaction. We present here the observational data on 10 Leonid meteors photographed during the 2002 Leonid storm. The intrinsic value of our orbital data lies in the fact that they are the first reduced orbits of the storm associated with the dust trail ejected from 55P/Tempel–Tuttle in 1767. In addition, our observational data allow us to compare the derived orbital elements with the theoretical data as a good test to check the quality of double-station photographic observations.

2. Observations, reduction, and methodology

The measurements were made during the night of November 18–19, 2002 by the Spanish Photographic Meteor Network, SPMN (Trigo-Rodríguez et al., 2001), from three stations located in Catalonia, where multi-station work was planned. Another station was in Andalusia, more precisely in the Calar Alto Observatory, from which video CCD records were obtained in order to derive the flux density of the shower. Table 1 provides the geographic location and height

Table 1
Observing stations

Station (province)	Longitude	Latitude	Height (m)	Observing technique
Barcelona	2°09′19″ E	41°27′43″ N	25	Video
Calar Alto (Almería)	2°10′11″ W	37°13′25″ N	2165	Video
Figueres (Girona)	2°44′42″ E	42°23′49″ N	510	Photographic
Gualba (Barcelona)	2°31′43″ E	41°42′54″ N	300	CCD

of these stations. In each station several photographic cameras or low-scan CCD detectors with 50 to 35 mm optics equipped with rotating shutters were installed. Camera operators took time exposures with an accuracy of one second, while the time of occurrence of the bright meteors were taken by SPMN members from simultaneous visual observations.

The photographic negatives were developed and scanned at 2700 points per inch using a Kodak SprintScan scanner. We used PhotoFinish 4 software to make the astrometric measures of the star trails and the meteors. The astrometric measurements were then introduced into our *Network* software, which used the different images to provide the equatorial coordinates of the meteors with an astrometric accuracy of 0.005°. Our software also allows us to identify the same meteor from various stations by assuming the typical values of ablation height through an automated search on the database for meteors that appeared during the same observing interval. It allowed a quick identification of the different meteors registered from the different stations and the direct calculation of the atmospheric trajectory and radiant for each meteor. Our software, used to derive the velocity of the meteoroid, takes into account the trajectory length and the number of shutter breaks. An averaged value of observed velocities for each shutter-break was assumed as the preatmospheric velocity V_∞, since the final deceleration is barely measurable for most cases. To determine orbital elements from our trajectory data we used the *MORB* program provided by Ceplecha et al. (2000) from the Ondrejov Observatory in the Czech Republic.

To obtain the most accurate astrometry of the photographic, video CCD and low-scan CCD images, they were all reduced using the same software and procedure. To measure the position of the meteors on the digital images we performed all measurements on an arbitrary *XY*-axis using the *Microsoft Photo Editor* software application. Then star and meteor coordinates on the plates were introduced into our software, *Network*, which performed the astrometry following the procedure developed by Steyaert (1990) and, in addition, searched for common meteors from the different stations. This software modeled the trajectory and deduced the apparent radiant position of the meteors numerically and graphically (see Fig. 1). Finally, we used the program MORB to derive the heliocentric elements of Leonid meteoroids (Ceplecha et al., 2000)

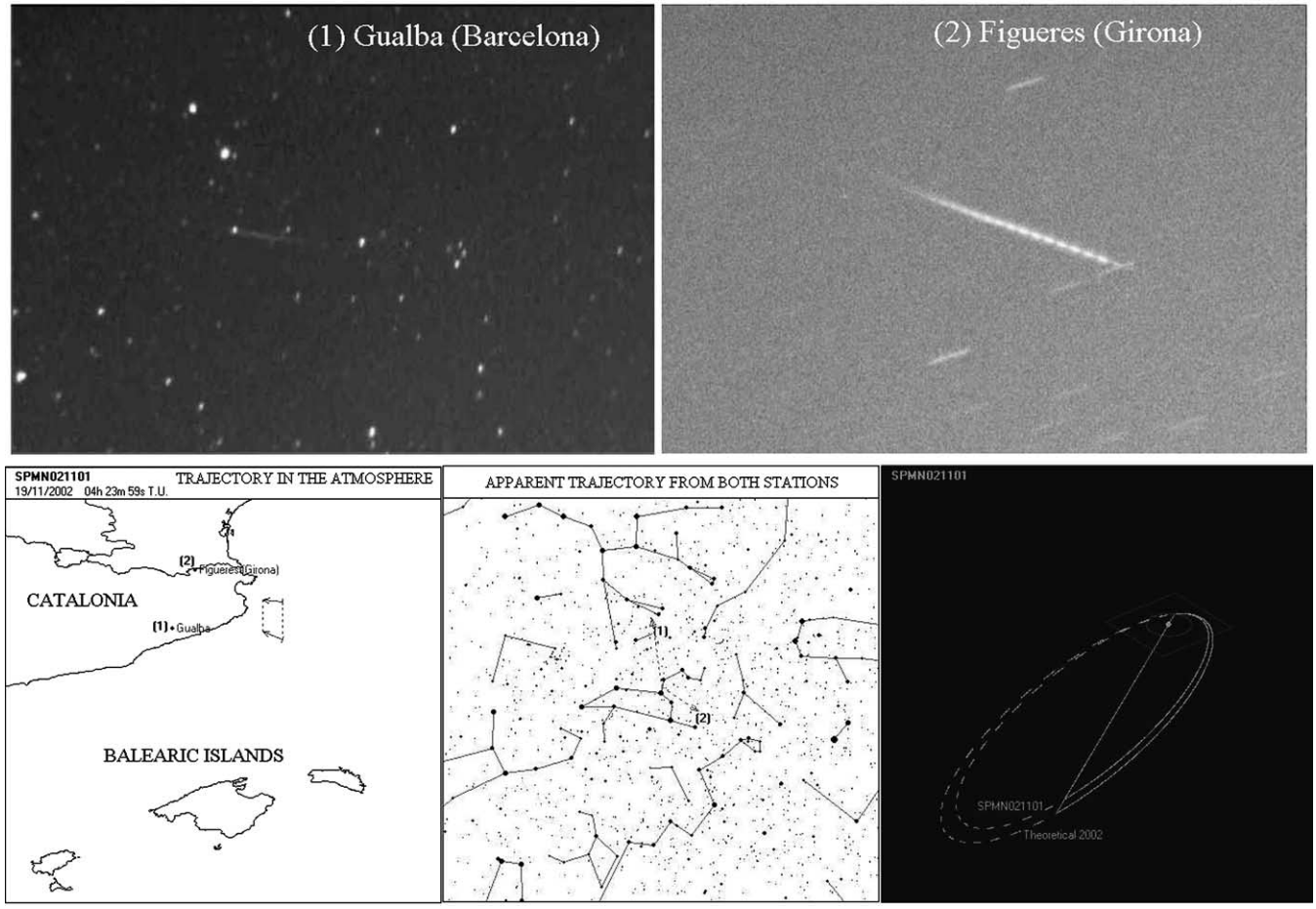

Fig. 1. Double-station meteor L2 from Gualba and Figueres stations. The software deduces the real trajectory in the atmosphere (left, below) from the apparent trajectory from both stations (center, below) and its heliocentric orbit compared with this derived theoretically for the 2002/7 revolution dust trail.

3. Trajectory data, radiants, and orbits

Using another software application developed by the SPMN team called *Photographic centers for multiple station meteor observations*, the different network nodes are able to derive the common center for each station depending on the geometry of meteor apparitions and the geographical coordinates of each station. During two hours of multiple station work, around 80 meteors were imaged from the different stations. Unfortunately, due to the reduced camera fields and different magnitude range, most of them were recorded only from single stations and, in consequence, it was not possible to derive trajectory and radiant data. Fifteen double-station meteors were clearly identified by our software. Figure 1 is an example of a double-station meteor, showing the stereographic images of Leonid L2 from two SPMN stations. From the apparent trajectory from both stations, our software determines the real trajectory into the atmosphere, the radiant and the heliocentric orbit of the associated meteoroid. Among the 15 precisely reduced meteors, 11 had convergence angles greater than 20°. The convergence angle (Q) is the angle between the two planes delimited by the observing sites and the meteor path in the triangulation. From these eleven meteors, in the end we only performed a detailed study of ten of them because the other one showed a large radiant dispersion (caused probably by its appearing close to the corner of the image where the astrometry is more imprecise) and was finally removed. The trajectory data of these accurately reduced meteors are given in Table 2, which shows the code system used for identification, apparent visual magnitude (M_v), the meteor trail beginning and end height on the Earth's surface (H_b and H_e in km), the geocentric radiant coordinates (α_g and δ_g to Eq. (2000.00)) and the velocity in km/s (at the top of atmosphere, geocentric and heliocentric). In order to determine the apparent radiant in the sky we prepared Fig. 2, where all fifty single-station meteors with accurate astrometry registered from the Gualba and Figueres stations have been included. In this figure it is clear that all meteors radiated from a very well defined radiant in R.A. $= 154.3° \pm 0.2°$ and Dec $= +21.6° \pm 0.1°$.

From the radiant position, apparition time and velocities estimated for these ten Leonid meteors that appeared over Catalonia we derived the orbital elements listed in Table 3. Unfortunately, bad weather in Andalusia forced us to reduce the double-station work to only 15 minutes under partially cloudy conditions, making it difficult to obtain additional orbits from this part of our network.

For comparison, Table 4 gives the averaged geocentric radiant and orbital elements obtained in this work compared to the theoretical values and those deduced by our team for the 1999 storm. The data in Table 4 show that the averaged values obtained from the 2002 Leonid storm meteors are similar to the theoretically derived values. In order to derive the 2002 orbit theoretically we used a previously tested integrator (Lyytinen and Jenniskens, 2003), which is based on a model that includes both the normal radiation pressure and a continuous acceleration term. This integrator package takes into account the radiation pressure that was decreased by a proper value to get just the desired original orbital period to reproduce the 2002 encounter. We used a sequence of test particles with the gravitation decreasing by a constant value between adjacent (in index) test particles. The typical

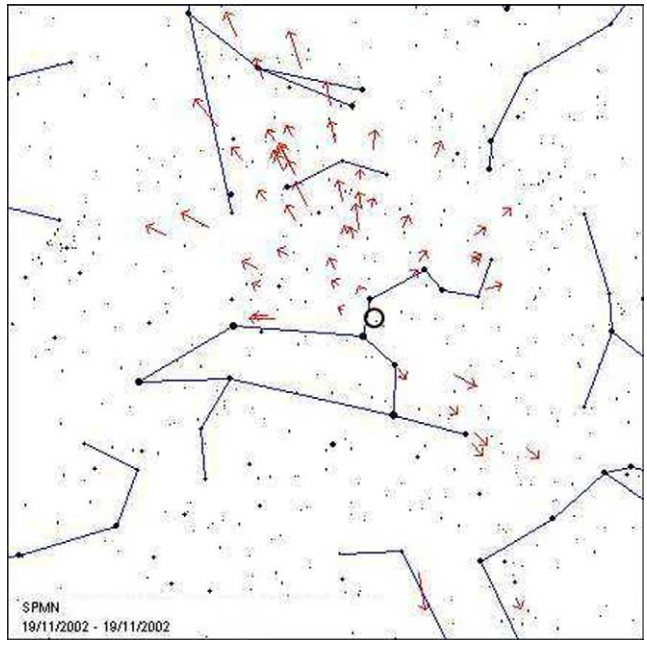

Fig. 2. Leonid 2002/7-rev radiant and apparent trajectories deduced from meteor astrometry.

Table 2
Visual magnitude, trajectory, geocentric radiant and velocity (at infinity, geocentric and heliocentric) for the multiple station recorded meteors

Code	M_v	H_b	H_e	α_g (°)	δ_g (°)	V_∞	V_g	V_h
L1	−3	114.7	96.7	154.55 ± 0.02	21.45 ± 0.03	71.6 ± 0.2	70.6	41.4
L2	−2	112.5	99.3	154.15 ± 0.03	21.40 ± 0.02	71.5 ± 0.2	70.4	41.2
L3	+1	105.8	103.1	153.49 ± 0.02	21.16 ± 0.02	71.7 ± 0.2	70.5	41.3
L4	0	116.3	102.7	154.09 ± 0.10	21.33 ± 0.02	71.5 ± 0.2	70.5	41.3
L5	+1	116.5	101.9	154.66 ± 0.02	21.83 ± 0.02	71.5 ± 0.2	70.5	41.3
L6	+1	105.7	101.8	153.71 ± 0.09	22.06 ± 0.03	71.6 ± 0.2	70.6	41.4
L7	−3	116.5	94.2	154.45 ± 0.11	21.43 ± 0.03	71.5 ± 0.3	70.5	41.3
L8	+1	112.6	105.3	154.25 ± 0.14	21.98 ± 0.03	71.8 ± 0.3	70.6	41.3
L9	−2	117.9	99.6	153.64 ± 0.06	21.31 ± 0.02	71.5 ± 0.2	70.3	41.1
L10	+2	113.7	108.2	154.53 ± 0.12	21.01 ± 0.02	71.7 ± 0.3	70.6	41.3

Table 3
Orbital elements of the 2002 Leonid storm meteoroids: Equinox 2000.00

Code	Q	a	e	i	ω	Ω
L1	0.98570 ± 0.00007	9.6 ± 1.7	0.896 ± 0.018	162.42 ± 0.05	173.94 ± 0.11	236.62862 ± 0.00001
L2	0.98655 ± 0.00006	9.2 ± 1.6	0.893 ± 0.018	162.72 ± 0.05	175.03 ± 0.10	236.62204 ± 0.00001
L3	0.98761 ± 0.00003	9.5 ± 1.7	0.896 ± 0.022	163.52 ± 0.05	176.86 ± 0.18	236.62413 ± 0.00001
L4	0.98669 ± 0.00022	10.2 ± 1.9	0.903 ± 0.018	163.48 ± 0.08	175.2 ± 0.3	236.6359 ± 0.0003
L5	0.98589 ± 0.00003	9.4 ± 1.7	0.896 ± 0.019	161.73 ± 0.05	174.2 ± 0.1	236.64391 ± 0.00001
L6	0.98785 ± 0.00011	10.3 ± 1.9	0.904 ± 0.018	161.96 ± 0.07	177.5 ± 0.3	236.65220 ± 0.0003
L7	0.98602 ± 0.00027	9.2 ± 1.6	0.892 ± 0.018	162.51 ± 0.09	174.3 ± 0.3	236.66372 ± 0.00016
L8	0.98696 ± 0.0031	9.5 ± 1.7	0.896 ± 0.018	161.73 ± 0.12	175.6 ± 0.5	236.6482 ± 0.0003
L9	0.98752 ± 0.00010	10.1 ± 1.9	0.902 ± 0.019	163.19 ± 0.19	176.7 ± 0.2	236.64751 ± 0.00001
L10	0.98518 ± 0.00036	9.7 ± 1.8	0.898 ± 0.018	163.15 ± 0.08	173.4 ± 0.4	236.62182 ± 0.00001
Mean	0.9866	9.8	0.897	162.7	174.7	–
St. Dev.	0.0009	0.6	0.005	0.7	1.8	–

Table 4
Comparison between the observed and theoretical radiant and main orbital elements

Storm	Radiant		Main orbital elements (2000.00)			
	R.A.	Dec.	q	a	I	ω
Leonids 2002	154.2 ± 0.4	$+21.5 \pm 0.3$	0.9866 ± 0.0009	9.8 ± 0.6	162.7 ± 0.7	174.7 ± 1.8
Theoretical 2002 7-revolution trail	154.49	+21.40	0.98590	10.29	162.56	174.04
Theoretical 2002 4-revolution trail	154.62	+21.33	0.98615	10.38	162.60	174.52
1999 Leonid	154.43 ± 0.6	$+21.83 \pm 0.4$	0.9838 ± 0.0002	9.6 ± 2.1	162.4 ± 0.7	172.4 ± 1.9

Data provided of the 1999 Leonid storm are taken from Trigo-Rodríguez et al. (2002).

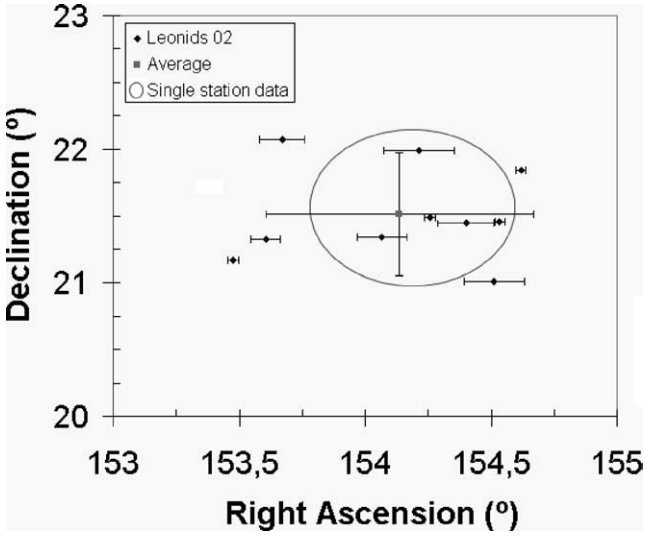

Fig. 3. Radiant position for the eleven double-station meteors (black points), averaged radiant for all them (square) and single-station derived radiant (open circle).

mass range of these test particles was taken to produce meteor magnitudes in the video and photographic range.

Figure 3 shows the radiant positions derived for the ten double-station meteors, their averaged position and dispersion, and the derived radiant position from the single-station meteor alignment shown in Fig. 2. The agreement between data is excellent. This figure clearly shows how some of our radiant data have large standard deviations in Right Ascension due to the intrinsic error associated with the time determination from visual observations. When camera operators observe the meteor directly the uncertainty can be in the order of 1 or 2 seconds, but for some meteors (e.g., L5, L7, L8, L9, and L11) the uncertainties are one order of magnitude larger. Fortunately, in the worst of cases the simultaneous low-scan CCD short time exposures allow the time of apparition to be defined within a maximum time interval of ± 22.5 seconds. In fact this must be the cause of the large standard deviation obtained in the radiant position and, consequently, in the longitude of ascending node. In the future, the best way to solve these problems is to use an all-sky intensified video camera to record the exact time of occurrence of the bright meteors (Betlem et al., 2000). This is the only way to determine the apparition time of all meteors with an accuracy of one second, especially during high meteor activity when visual identification can sometimes be unclear.

4. Derived Leonid flux densities

To derive the storm flux densities for different mass ranges we followed an identical procedure to the one presented previously in Trigo-Rodríguez et al. (2001). First, to obtain spatial densities from photographs, slow-scan CCD or video CCD imaging we need to know the real area that each image surveyed at the meteor level, depending on the camera field, altitude over the horizon and the population index of the meteor sample in the observational interval. We therefore use the methodology initially developed by Trigo-Rodríguez (1994) and later improved in several aspects by Bellot (1994). The photographic procedure consists in locat-

ing the longest edge of the photograph parallel to the horizon with a field center at an altitude above 45°. The reduced effective area $A_{\rm red}$ that collects meteoroids may be computed from Bellot (1994):

$$A_{\rm red} = \sum_i A_i \cdot r^{5\log(\frac{100\,\rm km}{d_i} - \varepsilon_i)}, \quad (1)$$

where A_i represents the projected geometrical area of a small portion of the photograph at distance d_i from the camera and extinction ε_i for meteoroids having a population index r estimated for each time interval. Note that the index i is such that all zones of the photograph enter the summation. For each photograph we obtain the corrected area depending on the field size, the altitude of the photographic center and the population index in the observational time interval.

To obtain the *limiting meteor magnitude* for each lens we performed simultaneous visual observations. We concluded from simultaneous visual and photographic observations (Trigo-Rodríguez et al., 2001) that a good estimation of the recorded limiting meteor magnitude is the following equation developed by Hawkins (1964):

$$m_{\rm meteor} = 2.512 \cdot \log\left(d^2 \cdot f^{-1} \cdot g\right) - 9.95, \quad (2)$$

where d is the effective aperture, f is the focal length of the lens, and g is the sensitivity of the emulsion stated in the international standard way of rating films (ISO).

We used an analog video camera Mintron 12V1C-EX based on the SONY Exview HAD ICX249AL chip with an objective with a 3.5 mm focal distance that covers a field of 86 × 66 square degrees. The effective limiting magnitude of this video CCD system is close to +3, as was deduced by considering the cumulative number of Leonids detected in the different magnitude ranges (Brown et al., 2002) and by visual comparison to stars in the field. In 104 minutes of effective observation, 491 meteors were registered, including 25 fireballs. The CCD observations made from Gualba (Barcelona) were taken with a 28 mm lens at f:2.8 on a CCD SX Starlight XPress that provides a limiting meteor magnitude close to +2.

To determine the spatial number density of meteoroids causing meteors of a generic magnitude M we used the method developed by Koschack and Rendtel (1990). On the basis of previous work the value of this generic magnitude M was taken as +6.5 for visual data, +3.5 for video data and −1 for photographic data (Trigo-Rodríguez et al., 2001). This is the reason why Table 5 shows the spatial number density of 2002 Leonids in the photographic magnitude range $]-\infty, -1]$ (here called $\rho_{-0.5}$) and video range $]-\infty, +3]$ (here called $\rho_{+3.5}$) compared to that obtained from visual data ($\rho_{6.5}$) in the range $]-\infty, +6.5]$. In order to deduce such spatial number densities, we first divided the selected observing periods into equal five-minute intervals. The second step was to derive the Zenital Hourly Rate (ZHR), which is the number of meteors from the shower an observer would see in one hour of net observing time under unobstructed skies with the radiant overhead and the faintest visible star in the field of view equal to +6.5. From the number of shower meteors (N) the Zenital Hourly Rate (ZHR) can be obtained

Table 5
Flux density for the 2002 Leonid storm

Interval UT	Mean λ_0 (°) 2000.0	$F_{\rm video}$	$N_{6.5}$	$\rho_{6.5}$	$N_{3.5}$	$r_{3.5}$	$\rho_{3.5}$	$N_{-0.5}$	$\rho_{-0.5}$
0300-0305	236.5689	–	7	220 ± 83	–	–	–	–	–
0305-0310	236.5727	–	8	270 ± 96	–	–	–	–	–
0310-0315	236.5765	–	7	220 ± 83	–	–	–	–	–
0315-0320	236.5800	1.43	5	160 ± 71	4	–	47 ± 24	3	19 ± 11
0320-0325	236.5835	1.25	4	230 ± 100	11	–	90 ± 27	5	21 ± 9
0325-0330	236.5874	1.33	3	300 ± 170	11	2.2 ± 0.6	94 ± 28	8	36 ± 13
0330-0335	236.5906	1.43	6	290 ± 120	15	–	140 ± 36	4	19 ± 10
0335-0340	236.5941	1.43	15	720 ± 190	17	–	150 ± 36	8	38 ± 23
0340-0345	236.5976	1.25	16	1200 ± 300	24	2.1 ± 0.4	190 ± 39	9	36 ± 12
0345-0350	236.6011	1.43	33	1600 ± 300	21	–	180 ± 39	6	28 ± 11
0350-0355	236.6047	1.53	61	2800 ± 400	28	2.0 ± 0.5	260 ± 49	7	34 ± 13
0355-0400	236.6082	1.43	92	2600 ± 400	47	–	400 ± 58	4	18 ± 9
0400-0405	236.6117	1.18	93	3300 ± 400	60	2.1 ± 0.4	340 ± 44	16	87 ± 22
0405-0410	236.6152	1.11	80	2300 ± 300	42	–	270 ± 42	9	25 ± 8
0410-0415	236.6223	1.11	50	1500 ± 300	38	2.2 ± 0.4	240 ± 39	12	40 ± 12
0415-0420	236.6259	1.25	22	1100 ± 300	25	–	180 ± 36	9	33 ± 11
0420-0425	236.6294	1.11	21	910 ± 200	29	1.9 ± 0.5	180 ± 33	9	30 ± 10
0425-0430	236.6329	1.18	17	800 ± 200	21	–	140 ± 31	6	21 ± 13
0430-0435	236.6365	1.18	15	530 ± 140	22	2.2 ± 0.6	140 ± 30	8	27 ± 10
0435-0440	236.6365	1.25	9	510 ± 170	21	–	140 ± 31	7	25 ± 9
0440-0445	236.6400	1.25	8	550 ± 190	8	–	55 ± 20	4	15 ± 8
0445-0450	236.6435	1.33	9	520 ± 170	16	1.9 ± 0.5	120 ± 30	7	27 ± 10
0450-0455	236.6470	1.67	10	440 ± 140	15	–	140 ± 36	2	10 ± 7
0455-0500	236.6505	2.5	7	310 ± 120	4	–	55 ± 28	2	14 ± 10
0500-0505	236.6540	cloudy	4	210 ± 105	–	–	–	–	–

as:

$$ZHR = \frac{N \cdot F \cdot r^{6.5-Lm}}{T \cdot \sin\theta}, \quad (3)$$

where the correction factor appears by limiting the magnitude consisting of the population index r of the shower in the selected interval and the limiting magnitude of the system Lm, the effective time of the interval T and the elevation of the shower radiant θ. Moreover in the preceding formula we also find F, a correction factor depending on the percentage of field covered by clouds (k):

$$F = \frac{100}{100 - k}. \quad (4)$$

In practice, this last factor was used only to correct the presence of clouds in the observing intervals registered by the Calar Alto video system because the stations in Catalonia had clear skies. Fortunately, the percentage of clouds during nearly all the observing intervals registered by the video system was below 20%. For more details we have included the correcting F_{video} value for each interval in Table 5. The presence of a full Moon was corrected by taking into account the limiting meteor magnitude Lm registered by each system under illuminated sky from simultaneous visual observations as in previous work (Trigo-Rodríguez et al., 2001). To improve the quality of the final results we considered only observing intervals with radiant elevations over 20° and a maximum global correction factor below 3.

Following the Koschack and Rendtel (1990) procedure we derive from the ZHR the number of meteoroids included in a cube with 1000 km-long edges in a third step using the equation:

$$\rho_{6.5} = \frac{ZHR \cdot C(r)}{3600 \cdot A_{\text{red}} \cdot v_g}, \quad (5)$$

where the ZHR appears corrected by a function $C(r)$ that depends on the population index and the probability of perception of each meteor of a particular magnitude. A_{red} is a standard area for which there is no extinction ε and the distance to the observer is assumed to be 100 km. To derive the spatial number densities included in Table 5 we used the same value of $C(r)$ derived previously by Koschack and Rendtel (1990). Additionally we used Eq. (1) in order to take into account the collected atmospheric volume covered by our video system (Bellot, 1994) in a similar way to how it had been performed previously (Trigo-Rodríguez et al., 2001).

This procedure enabled us to analyze the spatial flux density of the 2002 Leonid storm produced by the dust trail ejected from 55P/Tempel–Tuttle in 1767. The results are given in detail in Table 5 and plotted on Fig. 4, which shows the flux density profiles of the first peak of the 2002 Leonid storm (produced by the 1767 dust trail) for various particle populations. The study of these populations on a separate basis is interesting because they constitute different fractions of the full sample of meteoroids with particular evolution patterns. We can derive the mass associated with each meteor

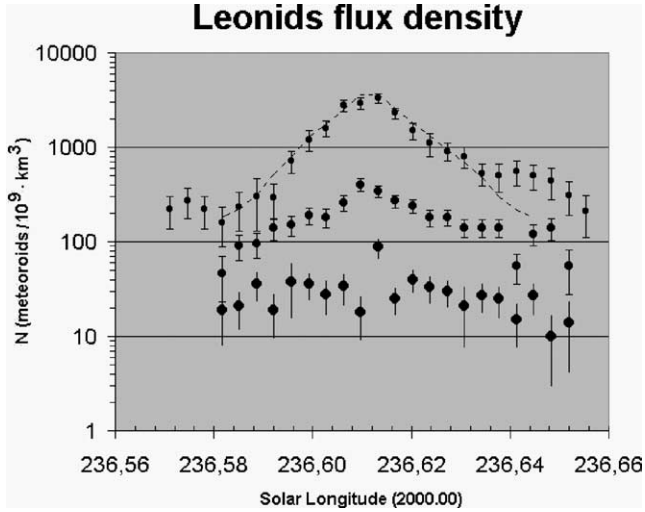

Fig. 4. Leonid flux densities derived from video observations for three ranges of masses (for more details see the text).

magnitude according to the formula (Verniani, 1973):

$$0.92 \cdot \log m = 24.214 - 3.91 \cdot \log V_g - 0.4 \cdot M_v, \quad (6)$$

where m is the meteor mass given in grams, M_v is the visual meteor magnitude and V_g is the geocentric velocity (in cm/s) of the meteoroids. According to this formula in Fig. 4 we have selected populations plotted at five-minute intervals. Small dots belong to particles causing meteors brighter than magnitude $+6.5$ (according to formula (6), heavier than 6×10^{-6} g), medium-sized ones represent a magnitude above $+3$ (heavier than 6×10^{-5} g), and big dots belong to -1 (heavier than 4×10^{-3} g). In Fig. 4 it is clear that the dust trail component is dominated by fairly faint meteors, the spatial number density for small particles being one order of magnitude greater than the one derived for medium-size meteoroids and two orders of magnitude greater than large-size meteoroids.

From these data, the spatial number densities (particles inside a cube with 1000 km-long edges) were derived for the first peak of the storm during the night of November 19, 2002. In Table 5 we compare the visual flux estimated from observations by SPMN members and those derived from video and CCD imaging during November 19th 2002. The error values are in the 66% confidence interval and were derived from the square of the number of observed meteors. Table 5 includes a cloud correction F_{video}, the spatial number density obtained from visual data ($\rho_{6.5}$), from video and CCD ($\rho_{3.5}$) and from photography ($\rho_{-0.5}$). One additional column called ($r_{3.5}$) includes the average population index values during the storm derived from the video recording. In order to obtain these values we compiled the magnitude distribution of video meteors in 15 minute intervals (0.01° in solar longitude). Although the intervals are too large to observe fast changes in the meteoroid population, the results show how the population index holds on a value of 2.2 ± 0.3 around the peak observed on the flux density profile. It is interesting to remark that although video data covers the

video magnitude range $]-\infty, +3]$ the derived population index values agree within error with those obtained recently from a large sample of visual observations by Arlt (2003).

5. Discussion

Multi-instrument observations allow data to be combined to derive the main characteristics of the 2002/7-revolution Leonid storm. Video data have provided us with detailed information on the population index and meteoroid flux density. During the storm, the population index remained quite stable, with values around $r = 2.2 \pm 0.3$. This result confirms preliminary 2002 Leonid MAC results (Jenniskens, 2002), and is consistent with the International Meteor Organization (IMO) visual results for this (Arlt et al., 2002) and previous storms (Arlt et al., 1999, 2001). This population index value is also similar to video observations of the 1999 storm (Gural and Jenniskens, 2000; Brown et al., 2002). The maximum spatial number density for particles producing meteors of +6.5 magnitude or brighter (in the following called $\rho_{6.5}$) during the storm was 3300 ± 400 meteoroids/10^9 km^3 for 5 min binning intervals (Table 5). This temporal resolution reveals a defined peak in flux lasting from approximately $\lambda_0 = 236.59°$–$236.64°$ (J2000.0).

It is remarkable that the spatial number density profile can be described with a small number of parameters, which allows comparison with other activity profiles, as previously noted Jenniskens (1995, 1996). According to this author, the activity profile can be fitted to an exponential curve as function of the solar longitude (λ_0):

$$\rho_{6.5} = \rho_{\max} \cdot 10^{-B|\lambda_0 - \lambda_{0\max}|}, \tag{7}$$

where the maximum spatial number density ($\rho_{\max}$), the slope B and the solar longitude of the maximum activity ($\lambda_{0\max}$) are free parameters. Following this approach we fitted the observed $\rho_{6.5}$ profile by plotting the result as the discontinuous curve in Fig. 4. It is interesting to remark that the best fit is obtained for a slope value of $B = (30 \pm 5)$ deg^{-1}, in full agreement with historical storms (Jenniskens, 1996). From this fit, we obtained the solar longitude of the peak of the distribution around $\lambda_0 = 236.612° \pm 0.001°$, which agrees within error with the observed IMO values (Arlt et al., 2002).

The single-station derived radiant in R.A. $= 154.3° \pm 0.2°$ and Dec $= +21.6° \pm 0.1°$ and the one derived from double-station meteors shown in Table 4 are perfectly compatible although, statistically, in the latter case the data sample is small. The reduced number of double-station meteors is probably not enough to observe a clustered radiant as was observed previously by Betlem et al. (2000). In any case, the standard deviations of the 2002 Leonid orbital parameters presented here are in the same magnitude order as those obtained in our previous work on the 1999 Leonids (Trigo-Rodríguez et al., 2002). Despite the relative low number of orbits obtained, principally as consequence of generalized bad weather in other areas of our network, seems significant that these are clearly linked to the specific perihelion return of the 55P/Tempel–Tuttle in 1767. From the solar longitude of the observed peak and the orbital elements is clear that the storm was produced by the predicted 7-revolution dust trail (Lyytinen and Van Flandern, 2000; McNaught and Asher, 2002). Of course, we cannot neglect the possibility that some of these bright meteoroids come from the so-called background component and have different orbital elements and release time, although the number of such meteors must be small. Such a component is associated with the presence of old particles dispersed within an annual stream. This translates into lower level activity superimposed on the dust trail activity that is usually present during Leonid storms (Jenniskens 1994, 1998).

Another interesting point to study in the future is the influence of radiation pressure on the Leonid meteoroids' orbital evolution. In an earlier study (Trigo-Rodríguez et al., 2002) we demonstrated the importance of radiation pressure β for orbital evolution for a sample of 1999 Leonid storm meteoroids. In this previous work we considered a typical value of $\beta = 0.001$ for a -2 magnitude Leonid meteoroid with a typical radius of 1×10^{-3} m and a density of 2 g/cm^3, identical to those proposed by Williams (1997) as being typical for visual Leonids. Although the structure and density of Leonid meteoroids are still partially unknown, several estimates of radius and density have recently been made (Rietmeijer, 2002). Although our 2002 Leonid sample is statistically small, if we compare the theoretical 7-revolution dust trail orbit with the averaged for these double-station meteors, the fit is good (taking into account the observational accuracy). To obtain the theoretical orbit we assumed a value of $\beta = 0.001$ as was found previously for the 1999 Leonid storm (Trigo-Rodríguez et al., 2002). This means that our data accuracy is capable of accounting for the effect of radiation pressure on the orbital evolution. But is it capable of showing the influence of other minor effects on orbital evolution? In order to answer this question Kimura et al. (2002) recently analyzed the dynamic effect of solar radiation on fluffy particles taking into account the light scattering effect and the equation of motion. The influence exerted by morphology, material composition and rotation on the evolution of interplanetary dust is also taken into consideration in the study and some interesting conclusions are reached. Considering the more than probable non-spherical shape of cometary meteoroids and the presence of chemical heterogeneity in the particles deduced from meteor spectroscopy (Borovicka et al., 1999; Trigo-Rodríguez, 2002; Trigo-Rodríguez et al., 2003, 2004), it would be reasonable to study the existence of orbital differences according to material composition and meteoroid mass in a large sample. Unfortunately, we consider this task to be impossible at this moment because the accuracy necessary to resolve orbital differences associated with these minor effects is unattainable from photographic or CCD observations using large

or medium focal distances. It is well known that there exists considerable uncertainty in determining the semimajor axis (a) from photographic observations due to uncertainties in velocity measurements. A small error in velocity usually leads to a significant error in a, as explained by Betlem et al. (1999), thus introducing a false dispersion in the orbital elements. In an earlier study we applied the "dust trail" theory to test the importance of improving the geocentric velocity measurements in the future by using larger focal distances and higher resolution video observations (Trigo-Rodríguez et al., 2002). Nowadays, the accuracy of the photographic orbital elements is in the order shown in Table 4, which is enough to compare the Poynting-Robertson influence on meteor orbits but probably below the precision required to deduce the influence of the minor effects studied by Kimura et al. (2002).

6. Conclusions

According to our results the 4 UT meteor storm of November 19, 2002 was produced by a dust trail ejected from the parent Comet 55P/Tempel–Tuttle in the return of 1767. The derived orbital elements belonging to the 2002/7-revolution meteoroids are very similar to one another, from which it can be deduced that they are associated with one single dust trail. The comparison between the mean orbital elements of the observed double-station meteoroids and the theoretical orbit for meteoroids ejected from this comet in 1767 has revealed good agreement between the orbits. In any case additional observational data would be useful in order to check the derived dispersion in the radiant and orbital elements from a statistically larger amount of data. Despite this it is significant that the theoretical orbit that best fits the observations must be determined by taking into account the radiation pressure typical for meteoroids producing meteors in the observed magnitude range. This result confirms our previous work on the 1999 Leonid storm where, taking into account the Poynting–Robertson effect, the match between observational and theoretical data is again extraordinarily good (Trigo-Rodríguez et al., 2002).

We also found radiant dispersions in the magnitude order previously determined for other Leonid storms (Betlem et al., 1999, 2000). Trajectory and single-station radiant data show a very conspicuous radiant that is less than 1 degree in diameter. The radiant position and size are similar to those obtained from double-station work but in the latter case the dispersion is larger, probably because the photographic data are not precise enough and the data sample is too small to define its real size. This would be caused by the greater astrometric uncertainties that are probably induced by joining photographic and CCD observations with different resolutions. In any case we have obtained a standard deviation in the same magnitude order as the one obtained previously during the 1999 storm (Trigo-Rodríguez et al., 2002).

Another important result is the high abundance of faint meteors deduced by comparing visual, video and photographic observations. This is predicted in theoretical models, as pointed out by Jenniskens (2002), probably because the smaller meteoroids have the highest surface-to-mass ratio and therefore the strongest impulse from gas drag during ejection from the comet's core and solar radiation pressure while they are in orbit. These faint meteors belonged to a narrow dust trail that the Earth crossed in approximately 1.0 ± 0.1 hours according to the fit of the spatial number density $+6.5$ included in Fig. 4. The maximum activity for this component of faint meteors coincided with those obtained from the other two populations in $\lambda_0 = 236.612^\circ \pm 0.001^\circ$. The spatial cross section of this dust trail, deduced from the duration of the storm, was approximately 0.1 million kilometers or 0.0007 ± 0.0001 A.U. Such a narrow flux profile agrees within error with the predicted duration of 1.2 hours derived by McNaught and Asher (2002) from the dust trail model.

Future studies of all available observations during this cometary return, obtained by different teams in an extraordinary international effort, will help increase our knowledge of the Leonid meteoroid stream. If we are to advance in the study of meteor storms with more reliable estimations of meteor flux densities, we will need to combine visual, photographic and video techniques. This probably will allow us to increase our knowledge about the distribution of meteoroid sizes in the trails which at present, is poorly understood. These advances will be especially important in order to estimate the storm intensities and develop more accurate predictions for future Leonid returns.

Acknowledgments

J.M.T-R. is grateful to the Spanish State Secretary of Education and Universities for a Postdoctoral grant. J.Ll. is grateful to MCYT for a Ramon y Cajal Research Program grant and to DURSI (Generalitat de Catalunya). J.L.O. acknowledges support from AE00-0169, AYA2001-4399-E, and AYA2002-0382. " FEDER funds are also acknowledged by J.L.O. We thank the reviews from David Asher and an anonymous referee that significantly improved this paper. The authors also thank F. Aceituno and J. Aceituno for assistance with the video recording during the 2002 Leonid storm at Calar Alto."

References

Arlt, R., Bellot Rubio, L., Brown, P., Gyssens, M., 1999. Bulletin 15 of the International Leonid watch: first global analysis of the 1999 Leonid storm. WGN, J. Int. Meteor Org. 27, 286–295.

Arlt, R., Kac, J., Krumov, V., Buchmann, A., Verbert, J., 2001. Bulletin 17 of the International Leonid watch: first global analysis of the 2001 Leonid storms. WGN, J. Int. Meteor Org. 29, 187–194.

Arlt, R., Krumov, V., Buchmann, A., Kac, J., Verbert, J., 2002. Bulletin 18 of the International Leonid watch: preliminary analysis of the 2002 Leonid meteor shower. WGN, J. Int. Meteor Org. 30, 205–212.

Arlt, R., 2003. Bulletin 19 of the International Leonid watch: population index study of the 2002 Leonid meteors. WGN, J. Int. Meteor Org. 31, 77–87.

Asher, D., 1999. The Leonid meteor storms of 1833 and 1966. Mon. Not. R. Astron. Soc. 307, 919–924.

Bellot, L., 1994. Spatial number densities and errors from photographic meteor observations under very high activity. WGN, J. Int. Meteor Org. 22, 118–130.

Betlem, H., Ter Kuile, C., van't Leven, J., de Lignie, M., Bellet, L.R., Koop, M., Angelos, C., Wilson, M., Jenniskens, P., 1997. Precisely reduced meteoroid trajectories and orbits from the 1995 Leonid meteor outburst. Planet. Space Sci. 45, 853–856.

Betlem, H., Jenniskens, P., Leven, J.V., Ter Kuile, C., Johannink, C., Zhao, H., Chenming, L., Guanyou, L., Zhu, J., Evans, S., Spurný, P., 1999. Precise trajectories and orbits of meteoroids from the 1999 Leonids meteor storm. Meteorit. Planet. Sci. 34, 979–986.

Betlem, H., Jenniskens, P., Spurný, P., Van Leeuwen, G.D., Miskotte, K., Ter Kuile, C.R., Zarubin, P., Angelos, C., 2000. Precise trajectories and orbits of meteoroids from the 1999 Leonid meteor storm. Earth Moon Planets 82–83, 277–284.

Borovicka, J., Stork, R., Bocek, J., 1999. First results from video spectroscopy of 1998 Leonid meteors. Meteorit. Planet. Sci. 34, 987–994.

Brown, P., 1999. The Leonid meteor shower: historical visual observations. Icarus 138, 287–309.

Brown, P., Arlt, R., 2000. Detailed visual observation and modelling of the 1998 Leonid shower. Earth Moon Planets 82–83, 419–428.

Brown, P., Campbell, M.D., Hawkes, R.L., Theijsmeijer, C., Jones, J., 2002. Multi-station electro-optical observations of the 1999 Leonid meteor storm. Planet. Space Sci. 50, 45–55.

Ceplecha, Z., Spurný, P., Borovicka, J., 2000. MORB Software to Determine Meteoroid Orbits. Ondrejov Observatory, Czech Republic.

Delsemme, 2000. Kuiper prize lecture cometary origin of the biosphere. Icarus 146, 313–325.

Gural, P., Jenniskens, P., 2000. Leonid storm flux analysis from one Leonid mac video AL50R. Earth Moon Planets 82–83, 221–249.

Hawkins, G.S., 1964. The Physics and Astronomy of Meteors, Comets and Meteorites. McGraw–Hill, New York.

Jenniskens, P., 1994. Meteoroid stream activity: I. The annual streams. Astron. Astrophys. 287, 990–1013.

Jenniskens, P., 1995. Meteor stream activity: II. Meteor outbursts. Astron. Astrophys. 295, 206–235.

Jenniskens, P., 1996. Meteor stream activity: III. Measurement of the first in a new series of Leonid outbursts. Meteorit. Planet. Sci. 31, 177–184.

Jenniskens, P., 1998. On the dynamics of meteoroid streams. Earth Planets Space 50, 555–567.

Jenniskens, P., Wilson, M.A., Packan, D., Laux, C., Krüger, C.H., Boyd, I.D., Popova, O.P., Fonda, M., 2000. Meteors: a delivery mechanism of organic matter to the Early Earth. Earth Moon Planets 82–83, 57–70.

Jenniskens, P., 2002. The 2002 Leonid MAC airbone mission: first results. WGN, J. Int. Meteor Org. 30, 218–224.

Kimura, H., Okamoto, H., Mukai, T., 2002. Radiation pressure and the Poynting–Robertson effect for fluffy dust particles. Icarus 157, 349–361.

Koschack, R., Rendtel, J., 1990. Determination of spatial number density and mass index from visual observations (I) and (II). WGN, J. Int. Meteor Org. 18, 44–58 and 119-140.

Kresak, L., 1993. Cometary dust trails and meteor storms. Astron. Astrophys. 279, 646–660.

Lindblad, B.A., Porubcan, V., Stohl, J., 1993. The orbit and mean radiant motion of the Leonid meteor stream. In: Stohl, J., Williams, I.P. (Eds.), Meteoroids and their parent bodies. Astron. Inst. of the Slovak Academy of Sciences, Slovakia, pp. 177–180.

Lyytinen, E., Van Flandern, T., 2000. Predicting the strength of Leonid outbursts. Earth Moon Planets 82–83, 149–166.

Lyytinen, E., Nissinen, M., Van Flandern, T., 2001. Improved 2001 Leonid storm predictions from a refined model. WGN, J. Int. Meteor Org. 29, 110–118.

Lyytinen, E., Jenniskens, P., 2003. Meteor outbursts from long-period comet dust trails. Icarus 162 (2), 443–452.

McNaught, R., Asher, D.J., 1999. Leonid dust trails and meteor storms. WGN, J. Int. Meteor Org. 27, 85–102.

McNaught, R., Asher, D.J., 2001. The 2001 Leonids and dust trail radiants. WGN, J. Int. Meteor Org. 29, 156–164.

McNaught, R., Asher, D.J., 2002. Leonid dust trail structure and predictions for 2002. WGN, J. Int. Meteor Org. 30, 132–143.

Milon, D., 1967. Great Leonid meteor shower of 1966. Sky Telescope 33, 4–10.

Rietmeijer, F.J.M., 2002. Shower meteoroids: constraints between interplanetary dust particles and Leonid meteors. Earth Moon Planets 88, 35–58.

Shiba, Y., Shimoda, C., Maruyama, T., Okumura, S., Tomita, M., Murasawa, A., Ohtsuka, K., Tomioka, H., Hidaka, E., 1999. Photographic observations of the 1996 Leonid fireballs in Japan. Earth Moon Planets 77, 47–54.

Simek, M., Pecina, P., 2000. Leonid meteor stream from Ondrejov radar observations in 1965–1967. Astron. Astrophys. 357, 777–781.

Simek, M., Pecina, P., 2001. Radar observation of the Leonids in 1998 and 1999. Astron. Astrophys. 365, 622–626.

Steyaert, C., 1990. Photographic Astrometry. Edited by the International Meteor Organization, Mechelan, Belgium.

Trigo-Rodríguez, J.M., 1994. Determination of spatial number density from photography. In: Roggemans, P. (Ed.), Proceedings of the 1993 International Meteor Conference. International Meteor Organization, Belgium.

Trigo-Rodríguez, J.M., 2000. The 1997 Leonid outburst. Astron. Astrophys. 355, 1160–1163.

Trigo-Rodríguez, J.M., Llorca, J., Fabregat, J., 2001. Leonid fluxes: 1994–1998 activity patterns. Meteorit. Planet. Sci. 36, 1597–1604.

Trigo-Rodríguez, J.M., 2002. Spectroscopic analysis of cometary and asteroidal fragments during its entry to the terrestrial atmosphere. PhD thesis. Publications of the University of Valencia. In Spanish.

Trigo-Rodríguez, J.M., Llorca, J., Fabregat, J., 2002. On the origin of the 1999 Leonid storm as deduced from photographic observations. Earth Moon Planets 91, 107–119.

Trigo-Rodríguez, J.M., Llorca, J., Borovicka, J., Fabregat, J., 2003. Chemical abundances from meteor spectra: I. Ratios of the main chemical elements. Meteorit. Planet. Sci. 38, 1283–1294.

Trigo-Rodríguez, J.M., Llorca, J., Fabregat, J., 2004. Chemical abundances from meteor spectra: II. Evidence for enlarged sodium abundances in meteoroids. Mon. Not. R. Astron. Soc. 348, 802–810.

Verniani, F., 1973. An analysis of the physical parameters of 5759 faint radio meteors. J. Geophys. Res. 78, 8429–8462.

Williams, I.P., 1997. The Leonid meteor shower: why are there storms but not regular annual activity? Mon. Not. R. Astron. Soc. 292, L37–L40.

Yeomans, D.K., Yau, K.K., Weissman, P.R., 1996. The impeding appearance of Comet Tempel–Tuttle and the Leonid meteors. Icarus 124, 407–413.

Wu, Z., Williams, I.P., 1996. Leonid meteor storms. Mon. Not. R. Astron. Soc. 280, 1210–1218.